HYDROLOGICAL PROCESSES
Hydrol. Process. **30**, 4384–4404 (2016)
Published online 2 August 2016 in Wiley Online Library
(wileyonlinelibrary.com) DOI: 10.1002/hyp.10922

Derivation and verification of empirical catchment response time equations for medium to large catchments in South Africa

O. J. Gericke,[1,2]* and J. C. Smithers,[2,3,4]

[1] *Unit for Sustainable Water and Environment, Department of Civil Engineering, Central University of Technology, Bloemfontein, Free State, South Africa*
[2] *Bioresources Engineering, School of Engineering, University of KwaZulu-Natal, Pietermaritzburg, South Africa*
[3] *Jeffares & Green (Pty) Ltd, 6 Pin Oak Avenue, Hilton, Pietermaritzburg, South Africa*
[4] *National Centre for Engineering in Agriculture, University of Southern Queensland, Toowoomba, Australia*

Abstract:

Despite uncertainties and errors in measurement, observed peak discharges are the best estimate of the true peak discharge from a catchment. However, in ungauged catchments, the catchment response time is a fundamental input to all methods of estimating peak discharges; hence, errors in estimated catchment response time directly impact on estimated peak discharges. In South Africa, this is particularly the case in ungauged medium to large catchments where practitioners are limited to use empirical methods that were calibrated on small catchments not located in South Africa. The time to peak (T_P), time of concentration (T_C) and lag time (T_L) are internationally the most frequently used catchment response time parameters and are normally estimated using either hydraulic or empirical methods. Almost 95% of all the time parameter estimation methods developed internationally are empirically based. This paper presents the derivation and verification of empirical T_P equations in a pilot scale study using 74 catchments located in four climatologically different regions of South Africa, with catchment areas ranging from 20 km^2 to 35 000 km^2. The objective is to develop unique relationships between observed T_P values and key climatological and geomorphological catchment predictor variables in order to estimate catchment T_P values at ungauged catchments. The results show that the derived empirical T_P equation(s) meet the requirement of consistency and ease of application. Independent verification tests confirmed the consistency, while the statistically significant independent predictor variables included in the regressions provide a good estimation of catchment response times and are also easy to determine by practitioners when required for future applications in ungauged catchments. It is recommended that the methodology used in this study should be expanded to other catchments to enable the development of a regional approach to improve estimation of time parameters on a national-scale. However, such a national-scale application would not only increase the confidence in using the suggested methodology and equation(s) in South Africa, but also highlights that a similar approach could be adopted internationally.

KEY WORDS catchment geomorphology; catchment response time; empirical methods; stepwise multiple regression analysis; time parameters

Received 20 November 2015; Accepted 12 May 2016

INTRODUCTION

Despite uncertainties and errors in measurement, observed peak discharges are the best estimate of the true peak discharge. Catchment response time is a fundamental input to all methods of estimating peak discharges in ungauged catchments; hence, errors in estimated catchment response time directly impact on estimated peak discharges (McCuen, 2009; Gericke and Smithers, 2014). The time to peak (T_P), time of concentration (T_C) and lag time (T_L) are the most frequently used catchment response time parameters and are normally estimated using either hydraulic or empirical methods, but analytical or semi-analytical methods are also sometimes used (McCuen *et al*., 1984; McCuen, 2009). The hydraulic methods are limited to the estimation of T_C under predominantly overland flow conditions and are best presented by either uniform flow theory or basic wave mechanics, for example, the kinematic wave (Henderson and Wooding, 1964; Morgali and Linsley, 1965; Woolhiser and Liggett, 1967), dynamic wave (Su and Fang, 2004) and kinematic Darcy–Weisbach approximations (Wong and Chen, 1997). In the case of empirical methods, the time parameters are related to the geomorphological, hydrological and meteorological parameters of a catchment using multiple regression analysis which

*Correspondence to: O. J. Gericke, Unit for Sustainable Water and Environment, Department of Civil Engineering, Central University of Technology, Free State, Bloemfontein, South Africa.
E-mail: jgericke@cut.ac.za

considers the whole catchment (overland and channel flows) and not only the sum of sequentially computed reach/segment behaviours as used in hydraulic methods (Kirpich, 1940; Watt and Chow, 1985; Papadakis and Kazan, 1987).

Empirical methods are the most frequently used by practitioners to estimate the catchment response time. Almost 95% of all the methods developed internationally are empirically based (Gericke and Smithers, 2014). However, the majority of these methods are applicable to and calibrated for small catchments, with only the studies of Johnstone and Cross (1949); Pullen (1969); Mimikou (1984); Watt and Chow (1985), and Sabol (2008) focusing on larger catchments of up to 5000 km^2. Only the T_L method proposed by Pullen (1969) was developed locally in South Africa (SA), while Schmidt and Schulze (1984) also derived equations to estimate T_L using data from 12 small agricultural catchments ($\leq$3.5 km^2) in SA and the United States of America (USA). The empirical Kerby (1959) and United States Bureau of Reclamation (USBR, 1973) equations are recommended for general use in SA to estimate the T_C for overland and channel flow conditions, respectively (SANRAL, 2013). However, both these equations were developed and calibrated in the USA for catchment areas less than 4 and 45 ha, respectively (McCuen *et al*., 1984). Despite the above limitations with the estimation of catchment response time at a medium to large catchment scale, it is not surprising that these time parameter estimation methods are commonly applied outside of their bounds, both in terms of areal extent and their original regions of development, without using any local correction factors.

The common practice used in empirical methods to relate time parameters to catchment characteristics using multiple regression analysis necessitate that any derived empirical equation must meet the requirement of statistical significance, consistency and ease of application, that is, inclusion of statistically independent catchment variables that are easy to determine by practitioners in ungauged catchments (McCuen, 2005; Gericke and Smithers, 2015). However, in order to identify suitable catchment predictor variables, their impact on catchment response time and the resulting runoff must be clearly understood, and it is necessary to consider all the catchment processes in a conceptual framework, consisting of three components: (i) the input (rainfall), (ii) the transfer function (catchment characteristics) and (iii) the output (excess rainfall/direct runoff). Catchment area is often identified as the single most important 'transfer function' as it demonstrates a strong correlation with many flood indices affecting the catchment response time (Pegram and Parak, 2004; McCuen, 2005). In addition to catchment area, other catchment variables such as hydraulic and main watercourse lengths, catchment centroid distance, average catchment and main watercourse slopes are regarded as equally important and should be considered as potential predictor variables (Kirpich, 1940; McCuen *et al*., 1984; Heggen, 2003; Gericke and Smithers, 2015).

The use of different independent catchment variables in a specific combination to predict the catchment response time could also have a negative impact on estimates. For example, differences in the estimates of the roughness and slope of catchments (overland flow) and main watercourses (channel flow), such as those based on the USBR (1973) equation which considers only the main watercourse characteristics, result in the underestimation of T_C on average by 50% (McCuen, 2009). Consequently, the resulting peak discharges will be overestimated by between 30% and 50% (McCuen, 2009). Bondelid *et al*. (1982) indicated that as much as 75% of the total error in design peak discharge estimates in ungauged catchments could be ascribed to errors in the estimation of empirical time parameters, while Gericke and Smithers (2014) also showed that the underestimation of time parameters by 80% or more could result in the overestimation of design peak discharges of up to 200%.

Apart from the catchment geomorphology, land-use and climatological variables also have an influence on the catchment response time. Simas (1996) used weighted Curve Number (*CN*) values as a land-use related variable to estimate lag times in small to medium catchments ($A \leq 15$ km^2). However, Gericke and Smithers (2015) argued that weighted *CN* values represent a linear catchment response and suggested that Mean Annual Precipitation (*MAP*) values should rather be used as a predictor variable to represent the regional rainfall variability which potentially has a larger influence on any non-linearity present in the catchment response. Internationally, the inclusion of climatological (rainfall) variables as predictor variables of catchment response time has, to date, been limited to the research conducted by Rao and Delleur (1974), Kadoya and Fukushima (1979); McCuen *et al*. (1984); Schmidt and Schulze (1984); Papadakis and Kazan (1987); Loukas and Quick (1996) and Gericke and Smithers (2015). However, only the research of Kadoya and Fukushima (1979) and Gericke and Smithers (2015) focussed on catchment areas larger than 20 km^2.

Given the sensitivity of design peak discharges in ungauged catchments to estimated catchment time parameter values as highlighted earlier, catchment response time at a medium to large catchment scale was identified as a potential research project to be included as part of the National Flood Studies Programme in SA (Smithers *et al*., 2014). Consequently, this not only served as a motivation for this study, but also emphasized that the continued use of such inappropriate time parameter estimation methods at these catchment scales both in SA and internationally (Grimaldi *et al*., 2012) limits the use of both event-based design flood estimation methods and advanced hydrological models when design peak discharges and associated volumes are estimated in ungauged catchments.

In considering the few international studies conducted at a medium to large catchment scale, the need for new and improved methodologies is clearly evident. In this paper, SA is used as case study area to investigate the estimation of catchment response times. The objectives of this study are to (i) derive empirical equations to estimate T_P, (ii) independently assess the performance of the derived equations, (iii) compare the results obtained against the widely used USBR equation and (iv) assess the impact of different estimates of catchment response time on the estimation of the design peak discharge. Data from 74 catchments located in four different climatological regions of SA, with catchment areas ranging from 20 to 35 000 km^2, are used in the study. The focus is on the use of multiple regression analysis to establish unique relationships between time to peak (T_{Px}) values estimated directly from observed streamflow data (Gericke and Smithers, 2016; submitted) and key climatological and geomorphological catchment predictor variables in order to estimate representative catchment T_P values at ungauged catchments.

A summary of the study area is contained in the following section, followed by a description of the methodologies adopted and the results obtained. This is followed by the discussion, conclusions and recommendations.

STUDY AREA

South Africa, which is located on the most southern tip of Africa (Figure 1), is demarcated into 22 primary drainage regions, that is, A to X (Midgley *et al*., 1994), which are further delineated into 148 secondary drainage regions, that is, A1, A2, to X4. In this study, 74 study catchments were selected in four different climatological regions (Figure 1). The four different climatological regions were defined according to the regionalization initially proposed by Alexander (2010). Hydrological and climatological information were used by Alexander (2010) to define nine distinctive climatological regions in SA. The four climatological regions in this study are situated in the Sub-tropical Lowveld, Highveld, Mediterranean and Eastern Escarpment regions. The four regions are also further defined by geographical location, altitude above mean sea level, rainfall type (convective, frontal and/or orographic), rainfall seasonality (summer, winter and/or all year) and average catchment slope classes (flat, moderate or steep).

This pilot study to identify the dominant hydrological processes influencing catchment response time is based on data from the four regions identified earlier and no further regionalization, for example, cluster analysis or region-of-influence (Burn, 1990; Zrinji and Burn, 1994; Hosking and Wallis, 1997; Ouarda *et al*., 2001; Guse *et al*., 2010), was undertaken. If the pilot study is successful, then regional approaches can be adopted when this approach is expanded to other catchments in SA. Both the geomorphological catchment characteristics and flood statistics will then be used to establish the regions and to test the homogeneity, respectively.

The layout of each region/catchment, river networks and locality of individual calibration and verification flow-gauging stations are shown in Figures 2(a) to (d).

The details contained in Appendix A of each region are summarized as follows:

(a) Northern Interior (NI): 17 catchments, with areas ranging from 61 to 23 852 km^2 and located in the A2, A3, A5 to A7 and A9 secondary drainage regions (Midgley *et al*., 1994), were selected in this Sub-tropical Lowveld and Highveld region which is predominantly characterized by summer rainfall. The *MAP* ranges from 348 to 2 031 mm (Lynch, 2004) and rainfall is characterized as highly variable. The topography is moderately steep with elevations varying from 544 to 1 763 m and with average catchment slopes between 3.5% and 21.6% (USGS, 2002).
(b) Central Interior (CI): 16 catchments, with areas ranging from 39 to 33 278 km^2 and extending across the C5 secondary drainage region (Midgley *et al*., 1994) were selected in this Highveld region which is predominantly characterized by convective rainfall during the summer months. The *MAP* ranges from 275 to 686 mm (Lynch, 2004). The topography is gentle with elevations varying from 1021 to 2120 m and with average catchment slopes ranging between 1.7% and 10.3% (USGS, 2002).
(c) Southern Winter Coastal (SWC): 19 catchments, with areas ranging from 22 to 2 878 km^2 and located in the G1, G2, G4, H1 to H4 and H6 to H7 secondary drainage regions (Midgley *et al*., 1994) were selected in this Mediterranean region. The *MAP* ranges from 192 to 1 834 mm (Lynch, 2004) and the winter rainfall is classified as either orographic and/or frontal rainfall. The topography is very steep with elevations varying from 86 to 2 060 m and with average catchment slopes ranging between 2.8% and 51.9% (USGS, 2002).
(d) Eastern Summer Coastal (ESC): 22 catchments, with areas ranging from 129 to 28 893 km^2 and located in the T1, T3 to T5, U2, U4, V1 to V3 and V5 to V6 secondary drainage regions (Midgley *et al*., 1994)

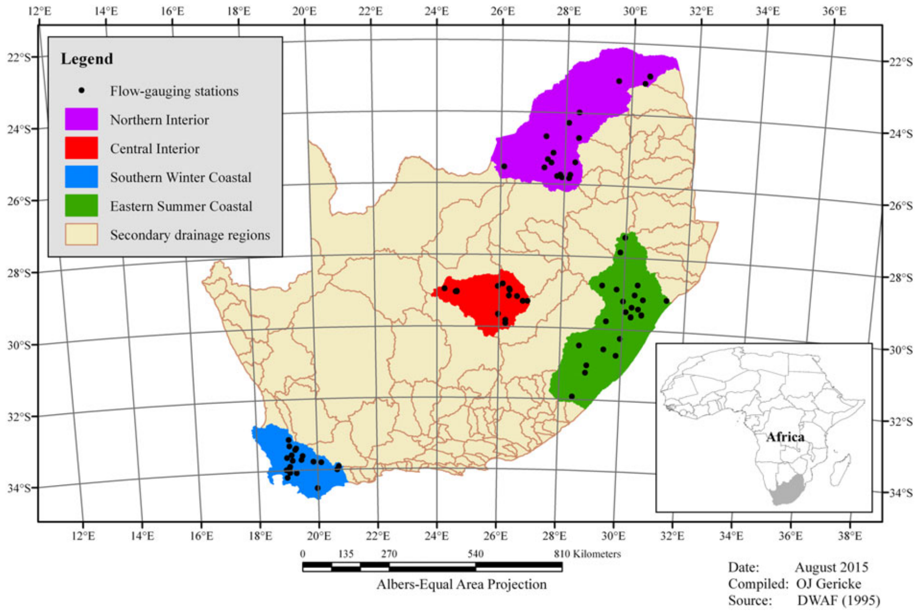

Figure 1. Location of the four climatological regions 296x210mm (300 x 300 DPI)

were selected in this Eastern Escarpment region which is predominantly characterized by all year and/or summer rainfall. The *MAP* ranges from 616 to 1 564 mm (Lynch, 2004). The topography is very steep with elevations varying from 31 to 3 149 m and with average catchment slopes ranging between 11% and 41.4% (USGS, 2002).

METHODOLOGY

This section provides the detailed methodology applied in the four climatologically different regions. The following procedures were performed: (i) identification and estimation of climatological variables (driving processes), (ii) determination of catchment variables and parameters using appropriate methods, including Geographical Information System (GIS) applications, (iii) derivation (calibration) and verification of the derived empirical time to peak (T_{Py}) equations, (iv) independent assessment of the performance of the T_{Py} equations in comparison with the observed catchment T_{Px} values (Gericke and Smithers, 2016; submitted), (v) comparison of the USBR equation (T_{Cy}) currently used as the 'recommended method' in SA with both the T_{Px} values and derived T_{Py} equations and (vi) translation of the various estimates of catchment response time into peak discharge to highlight the impact of these inconsistent time parameters on estimates of peak discharge.

The station numbers of the Department of Water and Sanitation (DWS) flow-gauging stations located at the outlet of each catchment are used as catchment descriptors for easy reference in all the tables and figures. Subscripts '*x*' and '*y*' are used to distinguish between observed data (*x*) and values estimated (*y*) using either the derived empirical T_{Py} equations (this study) or applying the currently 'recommended' USBR equation as commonly used in SA.

Estimation of climatological variables

The Isohyetal method was used to convert the individual *MAP* values (Lynch, 2004) at each rainfall station into average catchment values using the procedures as employed and recommended by Gericke and Du Plessis (2011). The 100-year design rainfall depth (P_{100}), associated with the critical storm duration (T_{Px}) in each catchment was estimated using the rainfall information and procedures as recommended by Alexander (2002).

Estimation of catchment variables

All the relevant GIS and catchment related data were obtained from the DWS (Directorate: Spatial and Land Information Management), which is responsible for the acquisition, processing and digitising of the data. The specific GIS data feature classes (lines, points and polygons) applicable to the four regions were extracted, projected and transformed from the original GIS data sets. All the geomorphological catchment characteristics [e.g. area (A), perimeter (P), hydraulic length (L_H), length of longest watercourse/river (L_{CH}), centroid distance (L_C), average catchment slope (S), average slope of main water course/river (S_{CH}) and drainage density (D_D)], were derived from a projected and transformed version of the Shuttle Radar Topography Mission Digital Elevation Model data for SA at 90-metre resolution (USGS, 2002).

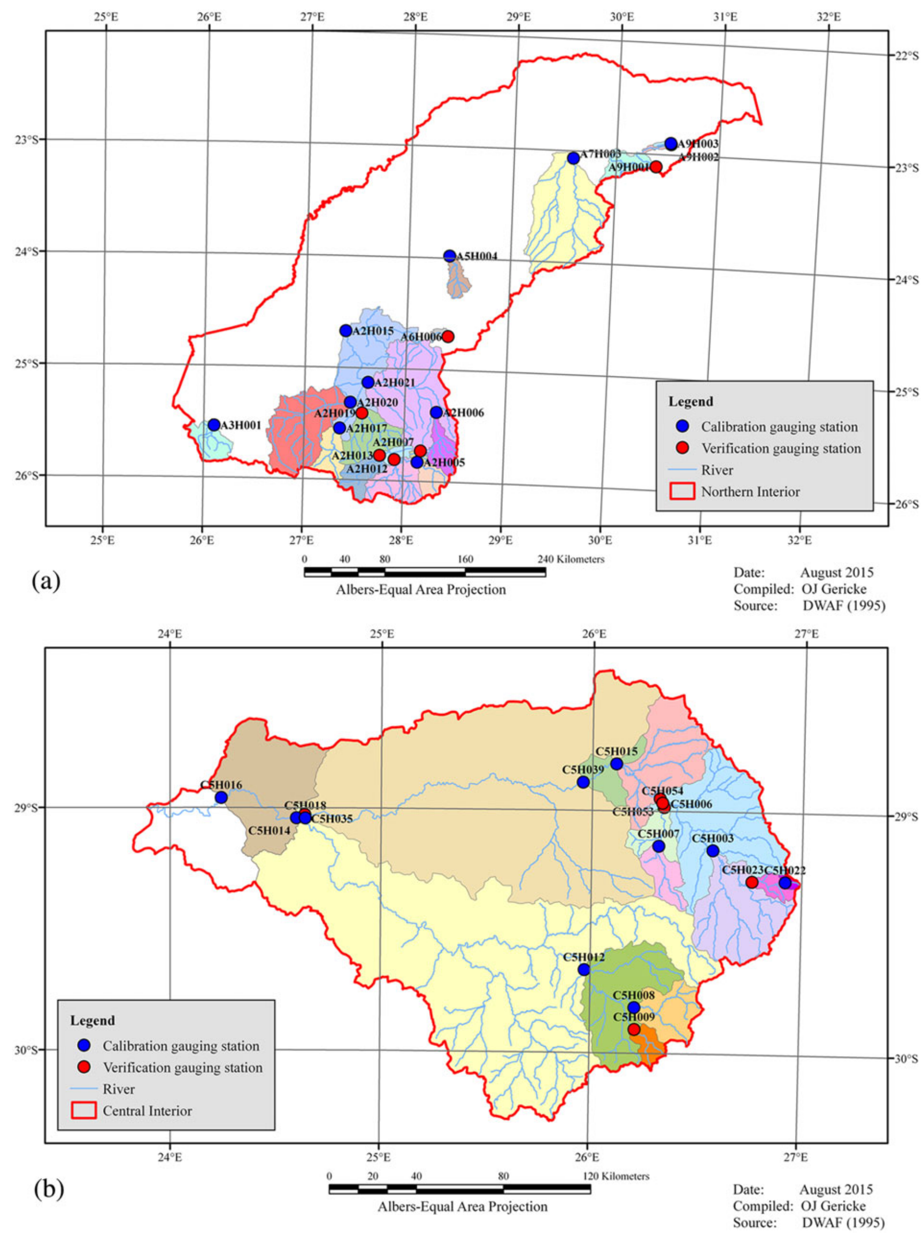

Figure 2. Layout and river gauging network of the (a) Northern Interior, (b) Central Interior, (c) SWC region, and (d) ESC region 296×210mm (300 × 300 DPI)

Owing to the high variability associated with the nature and distribution of landcover, vegetation, land-use, geology and soils at a medium to large catchment scale, the use of weighted *CN* values as representative independent variables to estimate time parameters was also included.

The general catchment attributes (e.g. climatological variables, catchment geomorphology, catchment variables and channel geomorphology) of each catchment in the four regions, are listed in Tables A1 to A4, Appendix A. The influences of each variable or parameter listed in these tables are highlighted where applicable in the subsequent sections.

The screening criteria (e.g. flow-gauging stations common to previous flood studies, record length, catchment area ranges and discharge rating tables), as used by Gericke and Smithers (2016; submitted) to establish the flood database to estimate the T_{Px} values from observed streamflow data, in conjunction with the location of each flow-gauging station in relation to other stations within a particular secondary drainage region, were used to select the flow-gauging stations used in this study. Forty-seven flow-gauging stations [denoted with * in Tables A1 to A4] were used for calibration, whilst the remaining 27 flow-gauging stations were used for independent verification of the empirical T_{Py} equations derived for each of the four

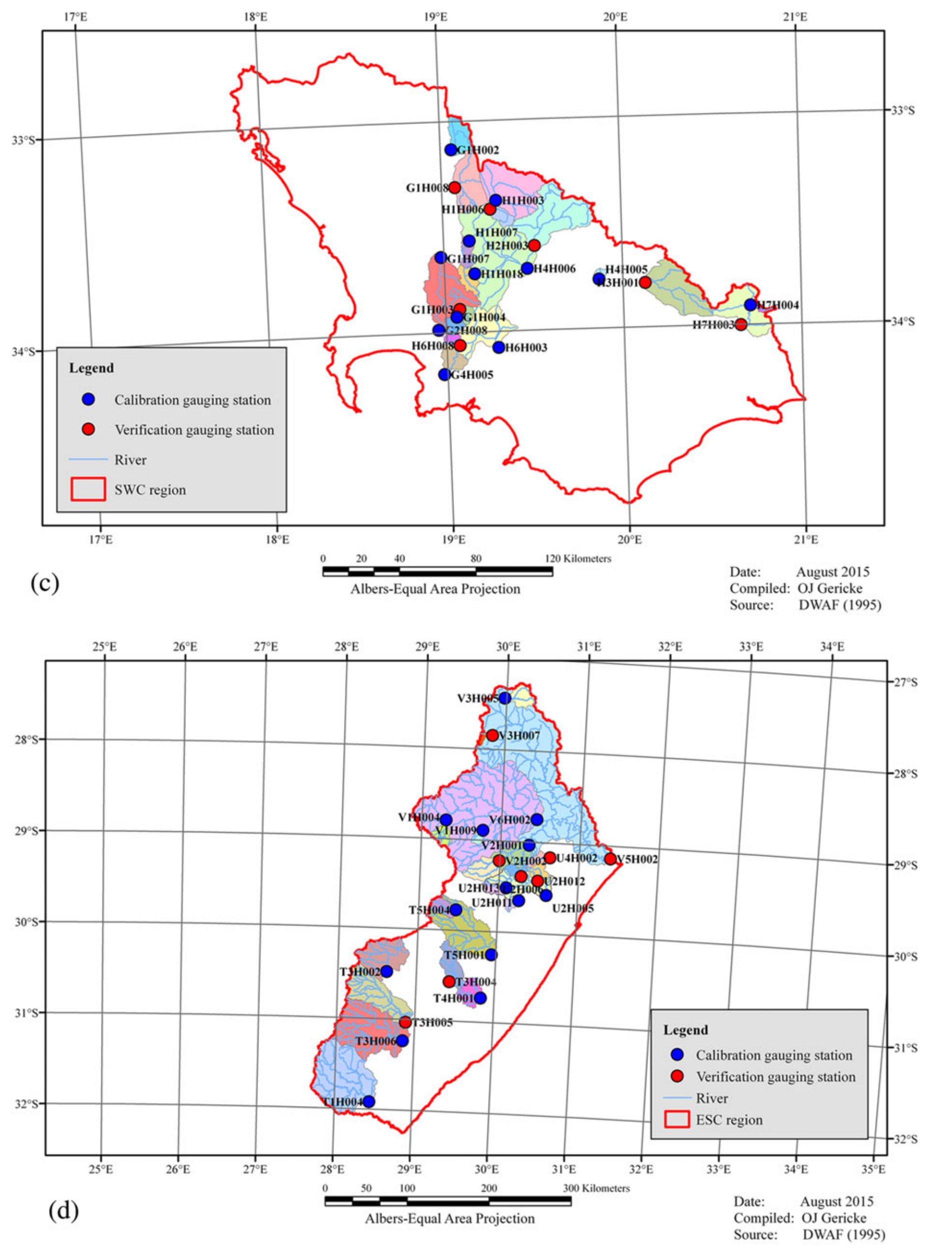

Figure 2. (Continued)

regions. Each catchment was carefully selected to ensure that the impact of upstream developments on flood propagation and the resulting catchment response time was minimized. In other words, catchments characterized by a high level of development and with non-pristine conditions, were not included in the study. In addition to the catchment screening criteria applied in this study, 87% of the selected study catchments were also used in previous flood studies (HRU, 1972; Hiemstra and Francis, 1979; Alexander, 2002; Görgens, 2007; and Görgens *et al.*, 2007), hence the selected catchments were deemed to be suitable for flood studies.

Observed stage levels exceeding the maximum rated stage at gauging weirs is a common problem in SA (Van der Spuy and Rademeyer, 2014). However, 92.7% of the flood hydrographs analysed in the 74 selected catchments were based on standard DWS discharge rating tables, that is, no extrapolation of the rating table was required. However, in cases where the observed flood levels exceeded the maximum rated flood level (H), the rating table was extrapolated by up to 20% using third-order polynomial regression analysis. The hydrograph shape, especially the peakedness as a result of a steep rising limb in relation to the hydrograph base length, and the relationship between observed event peak discharge (Q_{Pxi}) and associated direct runoff (Q_{Dxi}) value, were used as additional criteria to justify the rating table stage extrapolations (H_E) up to a 20% limit, that is, $H_E \leq 1.2H$. Typically, in such an event, the additional volume of direct runoff (Q_{DE}) due to the extrapolation was limited to 5%, that is, $Q_{DE} \leq 0.05\ Q_{Dxi}$; hence, any error made by using larger direct runoff volumes will have little impact on the sample statistics of the total flood volume. This approach was adopted in order to ensure samples of reasonable size, while the primary focus is on the time when the peak discharge occurs, and not just on the discharge value (Gericke and Smithers, 2016; submitted).

Calibration and verification of empirical T_P equations

The XLSTAT™ software (Addinsoft, 2014) was used to perform stepwise multiple regression analyses on the catchment time parameters and geomorphological catchment characteristics to establish calibrated relationships to estimate T_{Px}. The T_{Px} values used as dependent variables were determined by Gericke and Smithers (2016; submitted) from observed streamflow data using three different methods, that is, (i) duration of total net rise of a multi-peaked hydrograph, (ii) triangular-shaped direct runoff hydrograph approximations and (iii) linear catchment response functions. Methods (i) and (ii) are a measure of the observed time to peak values for individual flood events (T_{Pxi}), while Method (iii) represents the average catchment T_{Px}. Method (iii) was used in this study, as it proved to be the most consistent approach to estimate the average catchment T_{Px} values. Furthermore, it is also important to note that the use of Method (iii) provides only a single averaged catchment T_{Px} value as required for design flood estimation.

The following independent variables were considered for inclusion (Kirpich, 1940; McCuen *et al.*, 1984; Schmidt and Schulze, 1984; Simas, 1996; Pegram and Parak, 2004; McCuen, 2005; Gericke and Smithers, 2015): (i) A (km^2), (ii) P (km), (iii) L_H (km), (iv) L_{CH} (km), (v) L_C (km), (vi) S (%), (vii) S_{CH} (%), (viii) D_D (km km^{-2}), (ix) MAP (mm) and (x) weighted CN values.

Linear and Log-linear backward stepwise multiple regression analyses with deletion were used to remove the non-significant potential independent predictor variables (either in a normal and/or transformed format) at each step to minimize the total variation, while the included independent predictor variables were tested for statistical significance at a 95% confidence level. Hypothesis testing was performed at each step to ensure that only statistically significant independent variables were retained in the model, while non-significant variables were removed. Partial t-tests were used to test the significance of individual independent variables, while total F-tests were used to determine whether T_{Px} as a dependent variable is significantly correlated to the independent predictor variables included in the model (McCuen, 2005). A rejected null hypothesis [F-statistic of observed value (F) > critical F-statistic (F_α)] was used to identify the significant contribution of one or more of the independent variables towards the prediction accuracy. The Goodness-of-Fit (GOF) statistics were assessed using the coefficient of multiple-correlation [Equation 1] and the standard error of estimate [Equation 2] (McCuen, 2005). In addition to the assessment of GOF statistics, Equations 3 and 4 were also used as regression diagnostics to identify possible outliers and to estimate standardized residuals (Chatterjee and Simonoff, 2013).

$$R_i{}^2 = \frac{\sum_{i=1}^{N} (y_i - \bar{x})^2}{\sum_{i=1}^{N} (x_i - \bar{x})^2} \quad (1)$$

$$S_{Ey} = \left[\frac{1}{v}\sum_{i=1}^{N} (y_i - x_i)^2\right]^{0.5} \quad (2)$$

$$h_{ii} = \frac{1}{N} + \frac{(x_i - \bar{x})^2}{\sum_{i=1}^{N} (x_i - \bar{x})^2} \quad (3)$$

$$e_i = \frac{(y_i - x_i)}{S_{Ey}\sqrt{1 - h_{ii}}} \quad (4)$$

where R_i is the multiple-correlation coefficient for an equation with i independent variables, S_{Ey} is the standard error of estimate, h_{ii} is the i^{th} leverage value, e_i is the standardized residual, x_i is the observed value (dependent variable), $\bar{x}$ is the mean of observed values (dependent variables), y_i is the estimated value of dependent variable (x_i), i is the number of independent variables, N is the number of observations (sample size), and v is the degrees of freedom (N-i; with y-intercept = 0).

The performance of the calibrated empirical equation(s) was independently assessed at catchments not used during the calibration process, that is, the observed T_{Px} values were compared with the T_{Py} values estimated using the calibrated empirical equation(s).

Comparison of time parameter estimation results

In addition to the calibration and verification testing of the developed empirical equation(s), the 'recommended' USBR (1973) equation [Equation 5] currently widely used in SA to estimate T_{Cy} was also compared with both the observed (T_{Px}) and empirically estimated (T_{Py}) values, respectively. The estimates of T_C and T_P could be compared directly, because the conceptual definition of T_C equals T_P which is defined as the time interval between the start of effective rainfall and the peak discharge of a single-peaked hydrograph (McCuen *et al.*, 1984; McCuen, 2005; USDA NRCS, 2010), while Gericke and Smithers (2014, 2015) also showed that $T_C \approx T_P$ in medium to large catchments.

$$T_{Cy} = \left(\frac{0.87 L_H{}^2}{10 S_{CH}}\right)^{0.385} \tag{5}$$

where T_{Cy} is the estimated channel flow time of concentration (h), L_H is the hydraulic length of catchment (km), and S_{CH} is the average main river slope (%).

In order to highlight the impact of inconsistent results when translated into estimates of peak discharge, the 100-year design rainfall depths and catchment areas were used in the Standard Design Flood (SDF) method developed by Alexander (2002) to estimate design peak discharges in SA. The SDF method [Equation 6] is a regionally calibrated version of the Rational method and is deterministic-probabilistic in nature and applicable to catchment areas up to 40 000 km^2 (Alexander, 2002; Gericke and Du Plessis, 2012; SANRAL, 2013).

$$Q_{PT} = 0.278\left[\frac{C_2}{100} + \left(\frac{Y_T}{2.33}\right)\left(\frac{C_{100}}{100} - \frac{C_2}{100}\right)\right] I_T A \tag{6}$$

where Q_{PT} is the design peak discharge (m^3 s^{-1}), A is the catchment area (km^2), C_2 is the 2-year return period runoff coefficient, C_{100} is the 100-year return period runoff coefficient, I_T is the average design rainfall intensity (mm h^{-1}), and Y_T is the 100-year return period factor (2.33).

RESULTS

Calibration and verification of empirical T_P equations

The use of backward stepwise multiple linear regression analyses using untransformed data showed promising results; however, negative prediction values were evident in some of the calibration and verification catchments. In the case of transformed data, power-transformed ($y = ax^b$) independent variables, for example, A, P, L_C, L_H, $L_C L_H$ $(0.1S)^{-0.5}$ and $(L_C L_H)^{0.3}$, showed the highest degree of association ($r^2 \geq 0.8$) when individually plotted against the dependent variables (T_{Px} values) in most of the catchments. However, the transformed independent variables performed less satisfactorily when included as part of the multiple regression analyses in most of the catchments. Backward stepwise multiple Log-linear regression analyses with deletion generally resulted in the best prediction model.

The following statistically significant independent predictor variables were retained and included in the calibrated equation [Equation 7]: (i) *MAP*, (ii) A, (iii) L_C, (iv) L_H and (v) S. At a confidence level of 95%, the above independent variables contributed significantly towards the prediction accuracy in most or all of the regions, that is, L_C and S proved to be less significant in one or more region(s). However, the inclusion of these five independent variables proved to be the best combination of 'catchment transfer functions' to estimate the T_{Px} values at a catchment level. Hence, the same equation format, with different regional calibration coefficients was used in each of the four regions. The derived and simplified T_{Py} regression resulted in Equation 7:

$$T_{Py} = x_1{}^{MAP} x_2{}^{A} x_3{}^{L_C} x_4{}^{L_H} x_5{}^{S} \tag{7}$$

where T_{Py} is the estimated time to peak (h), A is the catchment area (km^2), L_C is the centroid distance (km), L_H is the hydraulic length (km), *MAP* is the Mean Annual Precipitation (mm), S is the average catchment slope (%), and x_1 to x_5 are regional calibration coefficients as listed in Table I.

Scatter plots of the T_{Py} [Equation 7] and average catchment T_{Px} values for both the calibration and verification catchments in each region are shown in Figure 3 to highlight any regional differences.

The moderate to high degree of association as depicted in Figure 3, not only confirmed the good correlation between T_{Px} and T_{Py}, but also the usefulness of Equation 7 to estimate the catchment response time in both the calibration and verification catchments. The overall r^2 value equals 0.79, while the individual regional r^2 values vary between 0.6 and 0.98. In considering the standardized residuals computed using Equation 4, it is evident that 96% of the total sample have standardized residuals less than ± 2. According to Chatterjee and Simonoff (2013), it is expected of a reliable regression model to have approximately 95% of the standardized residuals between −2 and +2, while standardized

Table I. Regional calibration coefficients applicable to Equation 7.

Region	Regional calibration coefficients [* 10^{-2}]				
	x_1	x_2	x_3	x_4	x_5
Northern Interior	100.280	99.993	99.865	101.612	91.344
Central Interior	100.313	99.984	106.106	98.608	98.081
SWC region	100.174	99.931	101.805	104.310	99.648
ESC region	100.297	99.991	99.594	101.177	97.529

ESC, Eastern Summer Coastal; SWC, Southern Winter Coastal.

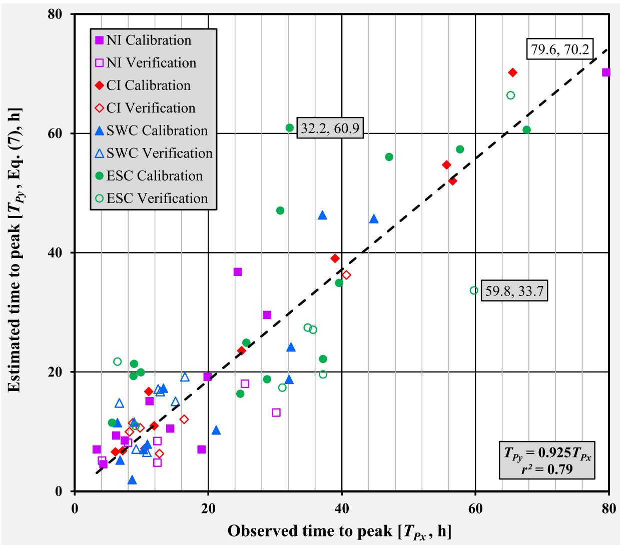

Figure 3. Scatter plot of the T_{Py} [Equation 7] and average catchment T_{Px} values at a catchment level in the four climatological regions. A linear trend line representative of the best fit (highest r^2 value) between the T_{Py} and T_{Px} values is shown. Data points characterised by T_{Px}-T_{Py} values with standardised residuals ≥ ± 2 are labelled in different colours, i.e. 'acceptable' leverage values (white fill) or outliers (grey fill) 259×175mm (96 × 96 DPI)

residuals ≥ ± 2 should be investigated as potential outliers. It is important to distinguish between 'acceptable' (T_{Py} is consistent with the regression relationship implied by the other T_{Px} values) and 'unacceptable' leverage values, that is, outliers. The T_{Px}-T_{Py} (79.6, 70.2) values in Figure 3 respresent 'acceptable' leverage values, while the remaining labelled T_{Px}-T_{Py} values are regarded as potential outliers, that is, 'unacceptable' leverage values which are inconsistent and which deviate from the regression relationship. By comparing these average catchment T_{Px} values with the T_{Py} values [Equation 7] in the four regions, the catchments in the CI demonstrated the best results with ±70% of the catchments showing < 20% differences between T_{Px} and T_{Py}. However, in the other regions, only ± 30% of the catchments are characterized by T_{Px}: T_{Py} ratio differences < 20%.

A summary of the GOF statistics and hypothesis testing results are listed in Table II.

The best results (Table II) were evident in the CI, with the standard error of the T_{Py} estimate = 4.1 h and an associated coefficient of multiple-correlation = 0.99. In acknowledging that 75% of the catchment areas in the CI are larger than 600 km^2, further emphasis is placed on the actual significance of the latter results, that is, the standard error results in each region must be clearly understood in the context of the actual travel time associated with the size of a particular catchment. The average regional T_{Px} values $\left(\overline{T_{Px}}\right)$ in the NI (18.3 h), CI (24.1 h), SWC (16.7 h) and ESC (32 h) regions could be used to benchmark these standard errors by considering the ratio of S_{Ey}: $\overline{T_{Px}}$ in each region, e.g. NI (0.46), CI (0.17), SWC (0.42) and ESC (0.45). Hence the comparable S_{Ey}: $\overline{T_{Px}}$ ratios obtained in the NI and ESC region, in conjunction with their similar R_i^2 values (≈0.85), highlight why the estimates in these two regions could be regarded as equivalent. It is also evident from Table II that, in all the regions, the rejection of the null hypothesis ($F > F_\alpha$) confirmed the significant relationship between T_{Px} and the independent predictor variables included in the regression model [Equation 7].

Table II. Summary of GOF statistics and hypothesis testing results applicable to both the calibration and verification catchments.

	T_{Py} [Equation 7] results			
Criterion/Region	NI	CI	SWC	ESC
Confidence level [(1−α), %]	95	95	95	95
Coefficient of multiple-correlation [Equation 1]	0.85	0.99	0.90	0.86
Standard error of estimate [Equation 2, h]	8.5	4.1	7.1	14.5
F-Observed value (F-statistic)	76.8	297.4	85.3	139.8
Critical F-statistic (F_α)	3.1	3.2	3.0	2.8

CI, Central Interior; ESC, Eastern Summer Coastal; GOF, Goodness-of-Fit; NI, Northern Interior; SWC, Southern Winter Coastal.

Comparison of time parameter and peak discharge estimation results

The impacts of estimating T_{Cy} [Equation 5] and T_{Py} [Equation 7] on the estimates of design peak discharge are investigated in this section. The relationship between the estimated (y) and observed (x) time parameter (T_Y/T_X) and design peak discharge (Q_Y/Q_X) ratios are shown in Figures 4(a) to (d).

The results illustrated in Figures 4(a) to (d) demonstrate the inverse relationship between peak discharge and catchment response time, that is, the underestimation of T_P (conceptual T_C) results in the overestimation of peak discharges and vice versa, viz. the overestimation of T_P results in underestimated peak discharges. Consequently, due to this inverse relationship and the time parameter results from each catchment, the worst peak discharge estimates are also expected in the catchments characterized by the poorest time parameter estimation results.

The T_{Cy} results illustrated in Figures 4(a) to (d) are characterized by several trends. Overall, 70% of the T_{Cy} values computed using the USBR equation [Equation 5] underestimated the T_{Px} values (denoted by T_Y/T_X ratio = 1) and showed a low to moderate degree of association with the observed T_{Px} values in the calibration and verification

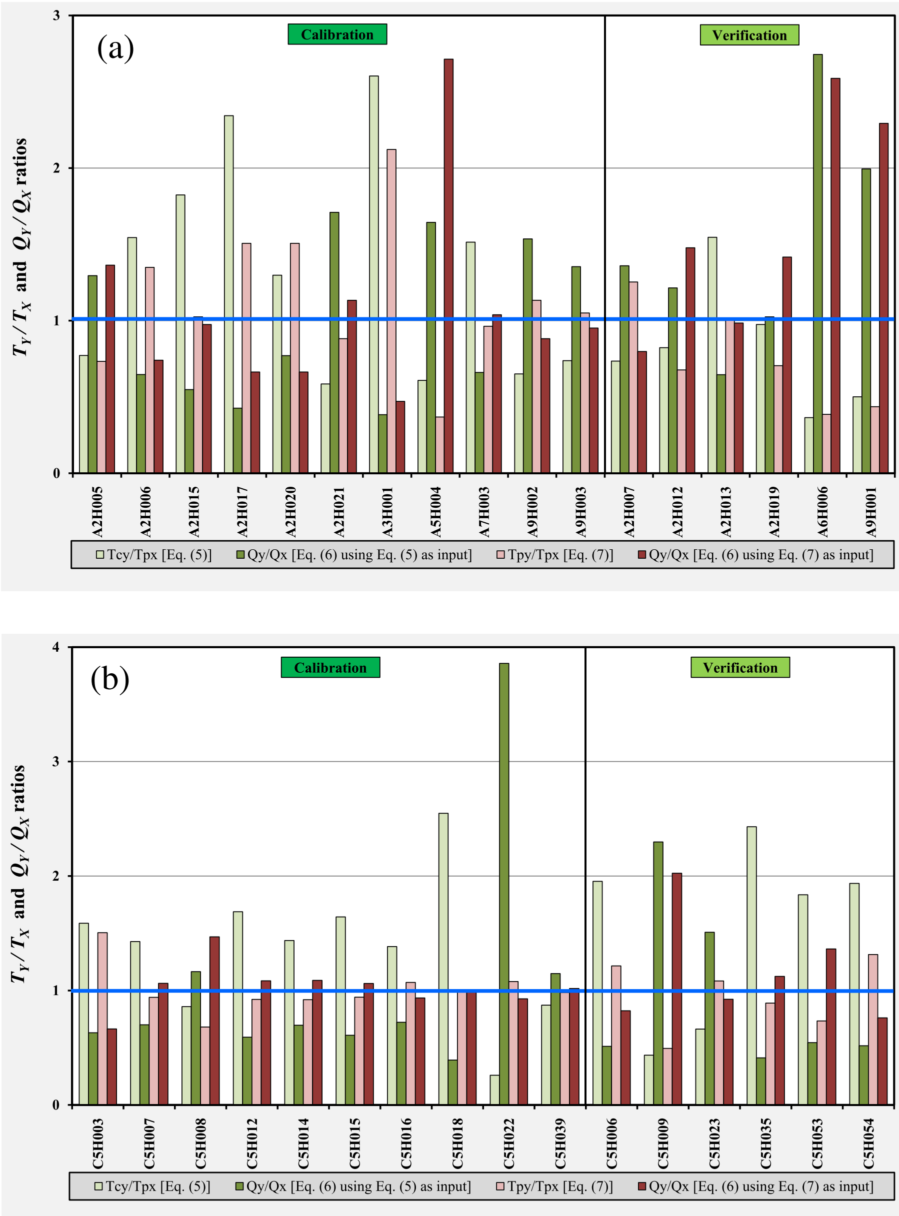

Figure 4. Inverse relationship between catchment response time and peak discharge illustrated using time parameter (T_Y/T_X) and peak discharge (Q_Y/Q_X) ratios for both the calibration and verification catchments in the (a) Northern Interior, (b) Central Interior, (c) SWC region, and (d) ESC region 256×174mm (96 × 96 DPI)

catchments. The r^2 values ranged from 0.56 to 0.75, while the T_{Cy} estimates varied between −93% and +160%. The poorest results were obtained in the SWC and ESC regions, with 90% of the T_{Cy} values being underestimated in comparison with T_{Px}. This was to be expected, as the latter two regions are characterized by much higher average S: S_{CH} ratios, which confirm the significant differences between the average catchment and main watercourse slopes in these regions. This is also in agreement with the findings of McCuen (2009), who showed that the USBR (1973) equation which considers only the main watercourse characteristics tends to underestimate T_{Cy} on average by 50% in catchments where significant differences in the roughness and slope of catchments and main watercourses are present. It also serves as an additional motivation why S is the preferred slope descriptor in all the catchments under consideration and is included as an independent predictor variable in Equation 7.

The T_{Py} estimations based on Equation 7 and illustrated in Figures 4(a) to (d), not only demonstrated a higher degree of association with T_{Px} in each region, but the underestimations and overestimations were also less significant when compared with the USBR

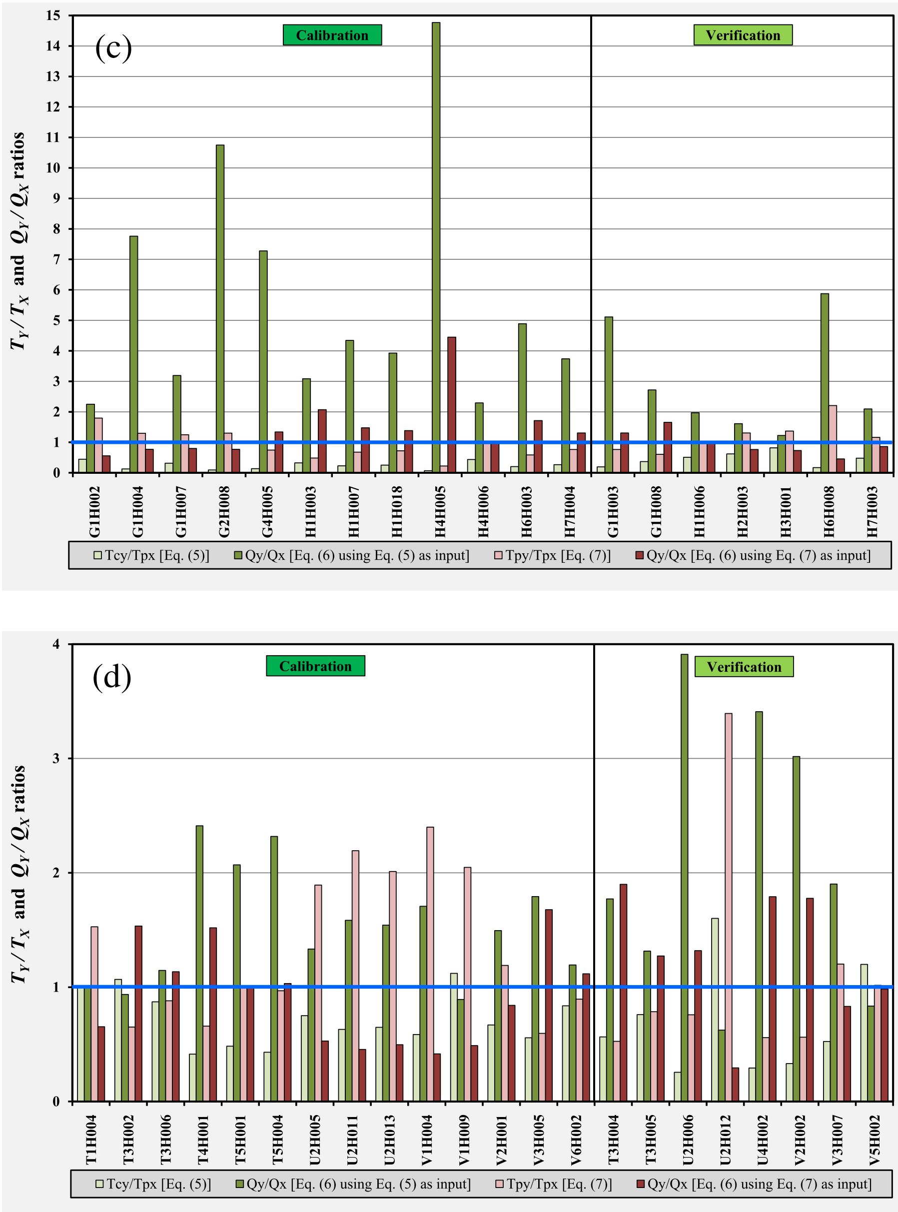

Figure 4. (Continued)

equation [Equation 5] in more than 70% of the catchments under consideration. Approximately 35% of the catchments under consideration had results in the 0.8–1.2 T_Y/T_X ratio range, that is, 20% underestimations or overestimations, while almost 70% of the T_{Py} estimates are within the 0.6–1.4 range. In applying Equation 7 in both the calibration and verification catchments, the degree of association (r^2 values) between the T_{Py} and T_{Px} values and associated underestimations and/or overestimations were as follows: (i) NI ($r^2 = 0.85$, −63% to +112%), (ii) CI ($r^2 = 0.97$, −50% to +50%), (iii) SWC region ($r^2 = 0.74$, −77% to +121%) and (iv) ESC region ($r^2 = 0.60$, −47% to +239%).

Typically, the overestimation of peak discharges by a ratio of 14 or more as evident in Figures 4(a) to (d) is associated with time parameter underestimations of up to −93%, while peak discharge underestimations of −70% are likely due to time parameter overestimations of up to +239%.

The hydrological processes and their association with specific catchment predictor variables which resulted in certain catchment response time estimates [Equation 7] and peak discharges [Equation 6], illustrated as time parameter (T_Y/T_X) and design peak discharge (Q_Y/Q_X)

Table III. Summary of the dominant hydrological processes and associated catchment predictor variables influencing the catchment response time and peak discharge.

Catchment parameter	Predictor variable(s) and/or other factors	Hydrological processes at a catchment/regional scale	Predictor(s) included in Equation 7
Size	Area (A)	Catchment area influences both catchment response time and the total volume of runoff. The high variability of T_{Pxi} (expressed as the %-difference between maximum and minimum T_{Pxi} values for individual flood events) in most of the catchments is regarded as being directly related and amplified by the catchment area, especially the influence which larger catchment areas have on the spatial distribution of catchment rainfall, as characterized by many rainfall events not covering the entire catchment. The T_{Pxi} variability was the lowest in the SWC region with $A \leq 2\,878\,km^2$, while the T_{Pxi} variability generally exceeded 90% for $A > 2\,500\,km^2$ in the NI. The spatial rainfall distribution in the CI and ESC region proved to be highly variable despite the catchment area under consideration. Peak discharge also proved to be proportionate to the square root of the catchment area.	A
Shape	Area (A) Perimeter (P) Centroid distance (L_C) Hydraulic length (L_H)	In wide, fan-shaped catchments the response time was shorter with higher associated peak discharges as opposed to in long, narrow catchments. In some of the 'circular catchments' in the NI and CI with a homogeneous slope distribution, the runoff from various parts of a catchment, tend to reach the outlet simultaneously. In elliptical catchments of comparable size in all the regions, the runoff is more distributed over time, thus resulting in longer catchment response times and lower peak discharges when compared with that of circular catchments. Differences of $\leq \pm 20\%$ between the T_{Py} values computed using Equation 7 and the average catchment T_{Px} values were associated with circularity ratios $[P/\sqrt{4\pi A}] < 1.5$ in all the regions. Average catchment shape parameters $[(L_C L_H)^{0.3}]$ between 9 and 11 (NI & SWC region) and > 17 (CI & ESC region) were also associated with $\leq \pm 20\%$ differences between T_{Py} and T_{Px}	A, L_C and L_H
Distance	Centroid distance (L_C) Length of longest river (L_{CH}) Hydraulic length (L_H)	The average catchment T_{Px} values were underestimated by $> 20\%$ at a catchment level in all the regions for L_C: L_H ratios < 0.5, hence the association between the shorter centroid distances and lower T_{Py} estimations computed using Equation 7.	L_C and L_H
Slope	Average catchment slope (S) Main watercourse slope (S_{CH})	Slopes, whether flat or steep, influence the catchment response time and hence the duration of the design rainfall and the resulting peak discharge and volume of direct runoff. The correlation between the average catchment and main watercourse slopes is comparable in the NI, CI and SWC region, that is, the average ratios of the slope descriptors (S: S_{CH}) varied between 12 and 20. However, in the ESC region the average S: S_{CH} ratio equals 32. After further examination of the S: S_{CH} ratios in the ESC region, it is evident that the catchments where the average T_{Px} values were underestimated by $> 20\%$ had higher average S: S_{CH} ratios (41) when compared with the other catchments where T_{Px} was overestimated, that is, S: $S_{CH} = 16$. This is to be expected, as shorter travel times are associated with steeper slopes.	S
Drainage density (D_D)	Area (A) Length of longest river (L_{CH}) Length of all other tributaries	Drainage density, that is, the ratio of the total length of watercourses within a catchment to the catchment area, could have a marked effect on the runoff rate. In the well-drained ($D_D > 0.3$) catchments, e.g. G1H002, G2H008 and H7H004	A

Continues

Table III. (*Continued*)

Catchment parameter	Predictor variable(s) and/or other factors	Hydrological processes at a catchment/regional scale	Predictor(s) included in Equation 7
		(SWC region) and U2H006 (ESC region), larger proportions of the rainfall contributed to direct runoff, while the catchment response times were comparatively shorter and hence resulting in steeper flood hydrographs. All the catchments in the NI and CI, with the exception of A2H007, A9H002, A9H003 and C5H003, are characterized by a relatively low drainage density, that is, $D_D \leq 0.20$. The catchments in the CI, and to a lesser extent the NI catchments, are also generally flatter with some surface depressions, hence the longer catchment response times and lower peak discharges.	
Rainfall	Mean Annual Precipitation (*MAP*) Rainfall intensity	At a medium to large catchment scale, *MAP* is preferred to rainfall intensity-related variables to represent regional variability. Fifty percent of the CI catchments could be regarded as 'semi-arid', with *MAP* values ≤ 465 mm, thus some of the infrequent occurring high intensity rainstorms resulted in more rapid (shorter) catchment responses and higher peak discharges. Conversely, in the wetter medium to large catchments of the SWC and ESC regions, that is, *MAP* values between 800 mm and 1400 mm, it could also be argued that the antecedent soil moisture status, the non-uniform distribution of rainfall and the attenuation of the resulting flood hydrograph as it moves towards the catchment outlet, are of more importance than the relationship between rainfall intensity and the infiltration rate of the soil.	*MAP*
	Type of rainfall	The convective rainfall in the NI and CI is generally of a short duration and high intensity, hence the shorter catchment response times and higher peak discharges. The orographic or frontal rain in the SWC region generally has a low intensity and long duration, and is controlled by the local topography, hence the longer catchment response times. In the ESC region, prolonged high intensity rainfall often resulted in shorter catchment response times when compared with similar-sized catchments in the other regions.	*MAP*
	Spatial and temporal distribution	The spatial distribution of rainfall determined the shape of the flood hydrographs. Rainfall occurring mainly in the upper reaches of a catchment is associated with a longer catchment response time, lower peak discharges and larger direct runoff volumes. On the other hand, high intensity rainfall near the catchment outlet resulted in a rapid catchment response time and a well defined peak. High intensity rainfall events, which gradually decrease to zero, typically resulted in flood hydrographs with a convex rising limb in the NI, CI and ESC region. Flood hydrographs with an upward concave rising limb were evident in some of the SWC catchments characterized by a gradual increase in rainfall from zero to a maximum, followed by no rainfall.	
Land-use, vegetation and soil characteristics	Weighted runoff curve number (*CN*)	At a catchment level, the nature and spatial distribution of main land-use groups could affect the volume, peak and temporal distribution of runoff. Because the 74 catchments under consideration are classified as 'rural pervious catchments', the impact of urbanization is insignificant, while the influence of natural vegetation on the volume of direct runoff and peak	None

Continues

discharges depends on the climatological region in which a particular catchment is situated. In the Mediterranean SWC and humid ESC regions, the effect of vegetal cover does not vary significantly between seasons. The vegetal cover in the NI and 'semi-arid' CI could vary appreciably, both seasonally and annually, thereby introducing more variability in the magnitude, timing and distribution of runoff, that is, the catchments response time and peak discharge.

CI, Central Interior; ESC, Eastern Summer Coastal; NI, Northern Interior; SWC, Southern Winter Coastal.

ratios in Figures 4(a) to (d), are summarized in Table III.

It is evident from Table III, that the use of different independent catchment variables in a specific combination to reflect the catchment response time should always be critically assessed to quantify whether any unique relationship could have a less desirable impact on estimations. The dominant hydrological processes as summarized in Table III are included as part of a conceptual framework in Equation 7, that is, the input (*MAP*), the transfer functions (A, L_C, L_H and S) and the output (Q). The importance of the catchment area as 'transfer function' and the affect thereof on catchment response time, are not only highlighted in Table III, but this is also in agreement with various other international studies (Kirpich, 1940; McCuen *et al*., 1984; Schmidt and Schulze, 1984; Simas, 1996; Pegram and Parak, 2004; McCuen, 2005). In the latter international studies, other 'transfer functions', e.g. L_C, L_H and S were also regarded as equally important.

DISCUSSION AND CONCLUSIONS

As highlighted in the Introduction, most of the time parameter estimation methods developed internationally are empirically based and applicable to small catchments. In SA, the T_L estimation methods developed locally by Pullen (1969) and Schmidt and Schulze (1984) are limited to small and/or medium catchments, while none of the recommended methods to estimate T_C were developed using local data. However, according to Gericke and Smithers (2014), the use of empirical time parameter equations applied beyond their original developmental regions and areal range and without the use of any local correction factors is widespread throughout many parts of the world. Hence, there is a need to develop a methodology to estimate catchment response times in medium to larger catchments.

The empirical equation(s) [Equation 7] derived and verified in this study, not only meet the requirement of statistical significance, consistency and ease of application by practitioners in ungauged catchments, but the use of the five retained independent predictor variables, improved the estimation of catchment response times and the resulting peak discharge. Furthermore, the inclusion of the average catchment slope is regarded as both conceptually and physically necessary to ensure that the other retained independent variables, that is, the catchment size (A) and distance (L_C and L_H) predictors provide a good indication of catchment storage effects (attenuation and travel time). The latter distance predictors are necessary to describe the shape of a catchment when considered in combination with the catchment area. The *MAP* included in Equation 7 incorporates the regional rainfall variability and typical antecedent moisture conditions, and the inclusion of *MAP* in Equation 7 is further justified by its statistical significance as independent predictor variable.

The significant impact of inconsistent time parameters on discharge estimates was clearly evident when these time parameters were used to estimate design peak discharges. Typically, time parameter overestimations and underestimations by ratios ranging between 1.4 and 0.1 respectively resulted in the underestimations and overestimation of peak discharges by ratios ranging between 0.3 and 15. Overall, the use of the derived empirical equation(s) [Equation 7] as input to the SDF method [Equation 6] resulted in improved peak discharge estimates in 60 of the 74 catchments under consideration. In approximately 40% of the catchments under consideration, the Q_Y/Q_X ratios using Equation 7 as input were within the 0.8–1.2 Q_Y/Q_X range, that is, 20% underestimations or overestimations in peak discharge.

However, Equation 7 also has some potential limitations, especially in terms of its application in ungauged catchments beyond the boundaries of the four climatologically different regions where it was developed. Therefore, the methodology followed in this study, in conjunction with the method to estimate T_{Px} as recommended by Gericke and Smithers (2016; submitted) should be expanded to other catchments in SA and internationally. This will enable the estimation of catchment response time parameters in medium to large catchments more confidently. In addition, adopting a regional approach will improve the robustness of the method and accuracy of the time parameter estimates.

Equation 7 also highlighted the inherent limitations and inconsistencies introduced when the USBR equation, which is currently recommended for general practice in SA, is applied outside its bounds without using any local correction factors. The T_{Py} estimations based on Equation 7, not only demonstrated a higher degree of association with T_{Px} in each region, but the underestimations and/or overestimations were also less significant in comparison with the estimates based on the USBR equation. Therefore, if practitioners continue to use inappropriate time parameter estimation methods, such as the USBR equation, then poor estimates of peak discharge are probable. In addition, potential future improvements in peak discharge estimation using both event-based and continuous simulation design flood estimation methods will not be realized, despite the current availability of other technologically advanced input parameter estimation methods, for example, GIS-based catchment parameters. In addition, not only will the accuracy of the above methods be limited, but it will also have an indirect impact on hydraulic designs, that is, underestimated time parameter values will result in over-designed hydraulic structures, and the overestimation of time parameters will result in under-designs.

Taking into consideration the significant influence time parameter values have on the resulting hydrograph shape and peak discharge, these newly derived empirical time parameter equations will ultimately provide improved peak discharge estimates at ungauged catchments in the four identified climatological regions of SA. Similarly, the method to estimate T_{Px}, as recommended by Gericke and Smithers (2016; submitted), should also be applied internationally in medium to large catchments to provide realistic observed catchment response times. This will not only enable the derivation of catchment-specific/regional empirical time parameter equations but would also add new knowledge and enhance the understanding of hydrological processes at these catchment scales.

FUTURE CHALLENGES

In view of the improved results obtained from this pilot study, the methodology should be expanded to other catchments in SA and internationally by taking cognisance of the following aspects:

(a) Regionalization: A regionalization scheme, for example, cluster analysis or region-of-influence (Burn, 1990; Zrinji and Burn, 1994; Hosking and Wallis, 1997; Ouarda *et al*., 2001; Guse *et al*., 2010) for catchment response time estimation in SA and/or internationally should be adopted or developed.
(b) Estimation of index catchment response times at ungauged sites: Once the method of regionalization has been selected, the methodology developed in this pilot study needs to be developed further. This will require the estimation of index (Dalrymple, 1960; Castellarin *et al*., 2005) time parameters at ungauged sites as a function of site characteristics, or the development of a means to transfer the hydrological information from gauged to ungauged sites within the newly identified regions.
(c) Assessment of the performance of the derived regional time parameter equations: In addition to the standard verification processes described and applied in this study, the empirical time parameter equations should also be independently tested in a selection of single-event or continuous simulation design flood estimation methods to verify the improved translation of

runoff volume into hydrographs and associated peak discharge estimates at a medium to large catchment scale. The 'improvement' in the translation of estimated time parameters into design peak discharges should be quantified by comparing the specific design estimates with at-site flood frequency analysis estimates. This will serve as the ultimate test of consistency, robustness and accuracy.

(d) Development of software interface: An interface to enable practitioners to apply and use the regionalized time parameter equations should be developed to enable the application of the proposed methodology both at a national-scale in SA and internationally.

It is envisaged that the implementation of both the identified research values and recommendations for future research, will ultimately contribute fundamentally to both improved time parameter and peak discharge estimations at a medium to large catchment scale in a regional context in SA. The suggested methodological approaches and recommendations for future research could also be adopted internationally to enhance the estimation of catchment response time parameters at these scales.

ACKNOWLEDGEMENTS

Support for this research by the National Research Foundation (NRF), University of KwaZulu-Natal (UKZN) and Central University of Technology, Free State (CUT FS) is gratefully acknowledged. We also wish to thank the anonymous reviewers for their constructive review comments, which have helped to significantly improve the paper.

REFERENCES

Addinsoft. 2014. XLSTAT software, Version 2014.6.05 [online]. Addinsoft, New York, USA. Available from: http://www.xlstat.com [7 January 2015].

Alexander WJR. 2002. The standard design flood. *Journal of the South African Institution of Civil Engineering* **44**(1): 26–30.

Alexander WJR. 2010. *Analytical Methods for Water Resource Development and Managment: Handbook for Prationers and Decision Makers*. Department of Civil and Biosystems Engineering, University of Pretoria: Pretoria. Available from: http://www.droughtsandfloods.com [5 February 2013].

Bondelid TR, McCuen RH, Jackson TJ. 1982. Sensitivity of SCS models to curve number variation. *Water Resources Bulletin* **20**(2): 337–349.

Burn DH. 1990. Evaluation of regional flood frequency analysis with a region of influence approach. *Water Resources Research* **26**(10): 2257–2265.

Castellarin A, Vogel RM, Matalas NC. 2005. Probabilistic behaviour of a regional envelope curve. *Water Resources Research* **41**: W06018. DOI:10.1029/2004WR003042

Chatterjee S, Simonoff JS. 2013. *Handbook of Regression Analysis*. Volume **5**, Wiley Handbooks in Applied Statistics. Hoboken, New Jersey: John Wiley and Sons Incorporated. DOI: 10.1002/9781118532843.

Dalrymple T. 1960. Flood frequency analyses. US Geological Survey Water Supply Paper 1543-A.

DWAF. 1995. GIS data: drainage regions of South Africa. Pretoria: Department of Water Affairs and Forestry.

Gericke OJ, Du Plessis JA. 2011. Evaluation of critical storm duration rainfall estimates used in flood hydrology in South Africa. *Water SA* **37** (4): 453–470.

Gericke OJ, Du Plessis JA. 2012. Evaluation of the standard design flood method in selected basins in South Africa. *Journal of the South African Institution of Civil Engineering* **54**(2): 2–14.

Gericke OJ, Smithers JC. 2014. Review of methods used to estimate catchment response time for the purpose of peak discharge estimation. *Hydrological Sciences Journal* **59**(11): 1935–1971. DOI:10.1080/02626667.2013.866712

Gericke OJ, Smithers JC. 2015. An improved and consistent approach to estimate catchment response time: case study in the C5 drainage region, South Africa. *Journal of Flood Risk Management* DOI:10.1111/jfr3.12206

Gericke OJ, Smithers JC. 2016. Direct estimation of catchment response time parameters in medium to large catchments using observed streamflow data. *Hydrological Processes*

Görgens AHM. 2007. Joint peak-volume (JPV) design flood hydrographs for South Africa. Pretoria: Water Research Commission; WRC Report No. 1420/3/07.

Görgens AHM, Lyons S, Hayes L, Makhabane M, Maluleke D. 2007. Modernised South African design flood practice in the context of dam safety. Pretoria: Water Research Commission; WRC Report No. 1420/2/07.

Grimaldi S, Petroselli A, Tuaro F, Porfiri M. 2012. Time of concentration: a paradox in modern hydrology. *Hydrological Sciences Journal* **57**(2): 217–228. DOI:10.1080/02626667.2011.644244

Guse B, Thieken AH, Castellarin A, Merz B. 2010. Deriving probabilistic regional envelope curves with two pooling methods. *Journal of Hydrology* **380**(1–2): 14–26.

Heggen R. 2003. Time of concentration, lag time and time to peak [online]. In *Proceedings, Application of Geo-informatics for Water Resources Management*, Shrestha B, Rajbhandari R (eds). International Centre for Integrated Mountain Development: Kathmandu, Nepal Ch. 3, 3.1–3.23. Available from: http://www.hkh-friend.net.np/rhdc/training/lectures/heggen/Tc_3.pdf [30 September 2010].

Henderson FM, Wooding RA. 1964. Overland flow and groundwater flow from a steady rainfall of finite duration. *Journal of Geophysical Research* **69**(8): 129–146.

Hiemstra LA, Francis DM. 1979. *The Runhydrograph: Theory and Application for Flood Predictions*. Water Research Commission: Pretoria.

Hosking JRM, Wallis JR. 1997. *Regional Frequency Analysis: An Approach Based on L-Moments*. Cambridge University Press, UK: Cambridge.

HRU. 1972. Design flood determination in South Africa. Johannesburg: Hydrological Research Unit, University of the Witwatersrand; Report No. 1/72.

Johnstone D, Cross WP. 1949. *Elements of Applied Hydrology*. Ronald Press: New York.

Kadoya M, Fukushima A. 1979. Concentration time of flood runoff in smaller river basins. In *Proceedings, 3rd International Hydrology Symposium on Theoretical and Applied Hydrology*, Morel-Seytoux HJ, Salas JD, Sanders TG, Smith RE (eds). Water Resources Publication: Fort Collins, Colorado; 75–88.

Kerby WS. 1959. Time of concentration for overland flow. *Civil Engineering* **29**(3): 174.

Kirpich ZP. 1940. Time of concentration of small agricultural watersheds. *Civil Engineering* **10**(6): 362.

Loukas A, Quick MC. 1996. Physically-based estimation of lag time for forested mountainous watersheds. *Hydrological Sciences Journal* **41**(1): 1–19. DOI:10.1080/02626669609491475

Lynch SD. 2004. Development of a raster database of annual, monthly and daily rainfall for Southern Africa. Pretoria: Water Research Commission; WRC Report No. 1156/1/04.

McCuen RH. 2005. *Hydrologic Analysis and Design*, 3rd edition. Prentice-Hall: New York.

McCuen RH. 2009. Uncertainty analyses of watershed time parameters. *Journal of Hydrologic Engineering* **14**(5): 490–498.

McCuen RH, Wong SL, Rawls WJ. 1984. Estimating urban time of concentration. *Journal of Hydraulic Engineering* **110**(7): 887–904.

Midgley DC, Pitman WV, Middleton BJ. 1994. Surface water resources of South Africa. Pretoria: Water Research Commission; WRC Report No. 298/2/94.

Mimikou M. 1984. Regional relationships between basin size and runoff characteristics. *Hydrological Sciences Journal* **29**(1, 3): 63–73.

Morgali JR, Linsley RK. 1965. Computer simulation of overland flow. *Journal of Hydraulics Division, ASCE* **91**(HY3): 81–100.

Ouarda TBMJ, Girard C, Cavadias G, Bobée B. 2001. Regional flood frequency estimation with canonical correlation analysis. *Journal of Hydrology* **254**(1–4): 157–173.

Papadakis KN, Kazan MN. 1987. Time of concentration in small rural watersheds. In *Proceedings, ASCE Engineering Hydrology Symposium*. ASCE: Williamsburg, VA; 633–638.

Pegram GGS, Parak M. 2004. A review of the regional maximum flood and rational formula using geomorphological information and observed floods. *Water SA* **30**(3): 377–392.

Pullen RA. 1969. Synthetic unit graphs for South Africa. Johannesburg: Hydrological Research Unit, University of the Witwatersrand; Report No. 3/69.

Rao AR, Delleur JW. 1974. Instantaneous unit hydrograph, peak discharges and time lags in urban areas. *Hydrological Sciences Bulletin* **19**(2): 85–198. DOI:10.1080/02626667409493898

Sabol GV. 2008. Hydrologic basin response parameter estimation guidelines. Scottsdale, Colorado: Dam Safety Report, Tierra Grande International Incorporated.

SANRAL. 2013. *Drainage Manual*, 6th edition. South African National Roads Agency Limited: Pretoria.

Schmidt EJ, Schulze RE. 1984. Improved estimation of peak flow rates using modified SCS Lag equations. Pietermaritzburg: Department of Agricultural Engineering, University of Natal; ACRU Report No. 17.

Simas MJC. 1996. Lag time characteristics in small watersheds in the United States. Thesis (PhD). University of Arizona.

Smithers JC, Görgens AHM, Gericke OJ, Jonker V, Roberts P. 2014. *The Initiation of a National Flood Studies Programme for South Africa*. SANCOLD: Pretoria.

Su DH, Fang X. 2004. Estimating travelling time of flat terrain by two-dimensional overland flow model. In *Shallow Flows*, Jirka GH, Uijttewaal WSJ (eds). : Rotterdam; 629–635.

USBR. 1973. *Design of Small Dams*, 2nd edition. Water Resources Technical Publications, United States Bureau of Reclamation: Washington, DC.

USDA NRCS. 2010. Time of concentration. In *National Engineering Handbook*, Woodward DE et al. (eds). United States Department of Agriculture Natural Resources Conservation Service: Washington, DC Ch. 15 (Section 4, Part 630); 1–18.

USGS. 2002. SRTM topography [online]. United States Geological Survey. Available from: http://dds.cr.usgs.gov/srtm/version2.1/SRTM/Document/Topo.pdf. [2 June 2010].

Van der Spuy D, Rademeyer PF. 2014. *Flood Frequency Estimation Methods as Applied in the Department of Water Affairs*. Department of Water Affairs: Pretoria.

Watt WE, Chow KCA. 1985. A general expression for basin lag time. *Canadian Journal of Civil Engineering* **12**: 294–300.

Wong TSW, Chen CN. 1997. Time of concentration formula for sheet flow of varying flow regime. *Journal of Hydrologic Engineering* **2**(3): 136–139.

Woolhiser DA, Liggett JA. 1967. Unsteady one-dimensional flow over a plane: the rising hydrograph. *Water Resources Research* **3**(3): 753–771.

Zrinji Z, Burn DH. 1994. Flood frequency analysis for ungauged sites using a region of influence approach. *Journal of Hydrology* **153**(1–4): 1–21.

APPENDIX A:

The catchment descriptors included in Tables A1 to A4 can be summarized as follows: (i) Mean Annual Precipitation (*MAP*), (ii) 100-year design rainfall depth (P_{100}), (iii) area (A), (iv) perimeter (P), (v) hydraulic length (L_H), (vi) centroid distance (L_C), (vii) average catchment slope (S), (viii) runoff Curve Number (CN), (ix) Standard Design Flood (SDF) runoff coefficients C_2 and C_{100}, (x) length of main watercourse (L_{CH}), (xi) average slope of main watercourse (S_{CH}) and (xii) drainage density (D_D).

Table A1. General information of the catchments situated in the Northern Interior

Catchment descriptor	A2H005*	A2H006*	A2H007	A2H012	A2H013	A2H015*	A2H017*	A2H019	A2H020*
Climatological variables									
MAP (mm)	673	686	706	682	658	626	652	661	603
P_{100} (mm)	157.5	151.2	131	153.6	144.8	190.2	141.1	181.1	178.1
Catchment geomorphology									
A (km^2)	774	1 030	145	2 555	1 161	23 852	1 082	6 120	4 546
P (km)	136	177	64	260	179	808	180	415	347
L_H (km)	51	86	17	57	64	252	76	132	176
L_C (km)	27	51	7	22	37	130	40	73	61
S (%)	2.73	4.76	6.52	5.30	7.03	5.13	7.43	5.78	5.31
Catchment variables									
Urban areas (%)	12.36	10.12	36.04	19.01	0.41	6.15	6.12	9.50	2.21
Rural areas (%)	25.02	76.06	32.77	36.07	85.24	80.32	92.61	68.22	96.92
Water bodies (%)	1.38	1.46	0.61	0.72	0.40	1.03	1.27	1.18	0.80
Weighted *CN* value	74.8	72.4	77.3	69.8	71.6	69.3	71.2	69.6	70.7
SDF C_2 coefficient	10	10	10	10	10	10	10	10	10
SDF C_{100} coefficient	40	40	40	40	40	40	40	40	40
Channel geomorphology									
L_{CH} (km)	48	86	17	57	57	251	76	132	176
Σ River lengths (km)	73	180	34	369	141	3110	132	876	621
S_{CH} (%)	0.44	0.39	1.47	0.69	0.52	0.19	0.49	0.36	0.34
Strahler order	2	2	2	3	2	5	2	3	3
Shreve magnitude	2	5	3	10	4	77	4	25	15
D_D (km km^{-2})	0.1	0.2	0.2	0.1	0.1	0.1	0.1	0.1	0.1

Catchment descriptor	A2H021*	A3H001*	A5H004*	A6H006	A7H003*	A9H001	A9H002*	A9H003*
Climatological variables								
MAP (mm)	611	566	623	630	433	827	1128	967
P_{100} (mm)	271.4	125.4	206.3	184.3	206.1	232.6	158	143
Catchment geomorphology								
A (km^2)	7 483	1 175	636	180	6 700	914	103	61
P (km)	459	174	140	63	396	186	76	44
L_H (km)	216	47	68	25	162	82	38	16
L_C (km)	70	17	37	9	79	44	19	11
S (%)	2.85	3.13	8.73	6.32	2.71	10.17	17.47	15.87
Catchment variables								
Urban areas (%)	9.11	0.48	0.00	1.84	4.58	3.41	8.44	17.71
Rural areas (%)	81.67	19.70	99.63	97.49	95.12	95.48	88.73	82.26
Water bodies (%)	1.32	0.57	0.37	0.66	0.30	1.11	2.83	0.03
Weighted *CN* value	69.7	68.9	63.6	61.1	61.5	68.4	68.5	70.8
SDF C_2 coefficient	10	10	5	5	5	5	5	5
SDF C_{100} coefficient	40	40	30	30	40	40	40	40
Channel geomorphology								
L_{CH} (km)	215	47	68	25	162	82	38	16
Σ River lengths (km)	947	149	124	25	625	145	38	16
S_{CH} (%)	0.19	0.73	0.71	1.10	0.33	0.50	2.01	1.16
Strahler order	4	3	2	1	3	2	1	1
Shreve magnitude	22	7	5	1	10	4	1	1
D_D (km km^{-2})	0.1	0.1	0.2	0.1	0.1	0.2	0.4	0.3

*= Flow-gauging stations used for the calibration of Equation 7

Table A2. General information of the catchments situated in the Central Interior

Catchment descriptor	C5H003*	C5H006	C5H007*	C5H008*	C5H009	C5H012*	C5H014*	C5H015*
Climatological variables								
MAP (mm)	552	515	495	451	464	440	433	519
P_{100} (mm)	130.2	129.1	128.8	130	130.8	130.5	187.6	147.7
Catchment geomorphology								
A (km^2)	1 641	676	346	598	189	2 366	31 283	5 939
P (km)	196	145	100	122	71	230	927	384
L_H (km)	71	64	41	41	24	87	326	160
L_C (km)	41	29	17	22	14	45	207	81
S (%)	3.90	2.02	1.75	4.83	3.66	3.28	2.13	2.77
Catchment variables								
Urban areas (%)	2.18	12.54	1.19	0.00	0.00	0.07	0.70	2.72
Rural areas (%)	95.09	85.91	97.57	99.11	98.83	98.78	95.93	95.17
Water bodies (%)	2.72	1.55	1.24	0.89	1.17	1.15	3.37	2.11
Weighted *CN* value	68.0	73.6	73.4	67.3	67.1	67.3	68.8	69.8
SDF C_2 coefficient	15	15	15	15	15	15	15	15
SDF C_{100} coefficient	60	60	60	60	60	60	60	60
Channel geomorphology								
L_{CH} (km)	71	64	40	41	24	87	326	160
Σ River lengths (km)	380	123	66	104	37	431	3320	1196
S_{CH} (%)	0.26	0.27	0.34	0.49	0.60	0.27	0.10	0.14
Strahler order	4	3	2	3	2	4	5	4
Shreve magnitude	14	7	3	5	2	18	102	42
D_D (km km^{-2})	0.2	0.2	0.2	0.2	0.2	0.2	0.1	0.2

Catchment descriptor	C5H016*	C5H018*	C5H022*	C5H023	C5H035	C5H039*	C5H053	C5H054
Climatological variables								
MAP (mm)	428	459	654	611	459	516	529	515
P_{100} (mm)	196.6	162.5	128.3	129.7	165.6	186.7	132.2	129.3
Catchment geomorphology								
A (km^2)	33 278	17 361	39	185	17 359	6 331	4 569	687
P (km)	980	730	28	65	730	411	329	146
L_H (km)	378	375	8	29	373	187	120	68
L_C (km)	230	174	3	17	173	103	56	33
S (%)	2.09	1.73	10.29	7.09	1.73	2.66	3.08	2.07
Catchment variables								
Urban areas (%)	0.66	1.18	0.00	0.02	1.18	2.55	3.42	12.34
Rural areas (%)	96.04	94.64	98.22	97.08	94.64	94.94	94.59	86.06
Water bodies (%)	3.30	4.18	1.78	2.90	4.18	2.51	1.99	1.60
Weighted *CN* value	69.0	70.1	67.8	67.9	70.1	69.8	69.8	73.6
SDF C_2 coefficient	15	15	15	15	15	15	15	15
SDF C_{100} coefficient	60	60	60	60	60	60	60	60
Channel geomorphology								
L_{CH} (km)	378	375	8	29	373	187	119	67
Σ River lengths (km)	3372	1617	8	37	1629	1236	937	127
S_{CH} (%)	0.10	0.08	1.70	0.58	0.08	0.13	0.18	0.26
Strahler order	5	4	1	2	4	4	4	3
Shreve magnitude	102	47	1	4	47	42	34	7
D_D (km km^{-2})	0.1	0.1	0.2	0.2	0.1	0.2	0.2	0.2

*= Flow-gauging stations used for the calibration of Equation 7

Table A3. General information of the catchments situated in the SWC region

Catchment descriptor	G1H002*	G1H003	G1H004*	G1H007*	G1H008	G2H008*	G4H005*	H1H003*	H1H006	H1H007*
Climatological variables										
MAP (mm)	729	915	1 392	899	586	1 345	1 065	452	455	673
P_{100} (mm)	62.3	69.6	80.2	141.3	73.8	68.8	170.4	135.1	120	108.1
Catchment geomorphology										
A (km^2)	186	47	69	724	394	22	146	656	753	80
P (km)	65	32	40	128	93	22	60	130	135	54
L_H (km)	28	10	14	56	26	6	30	39	47	19
L_C (km)	13	5	4	29	6	3	14	22	30	9
S (%)	33.53	28.88	52.31	26.21	18.89	51.76	20.71	16.41	21.20	40.69
Catchment variables										
Urban areas (%)	0.00	3.88	0.00	4.75	0.55	0.00	2.47	1.47	2.23	0.00
Rural areas (%)	99.99	95.67	99.84	93.86	98.44	100.00	94.00	95.97	96.49	100.00
Water bodies (%)	0.01	0.45	0.16	1.39	1.01	0.00	3.53	2.55	1.28	0.00
Weighted *CN* value	59.2	64.5	55.2	61.5	67.9	61.6	64.1	67.4	66.5	60.0
SDF C_2 coefficient	40	40	40	40	40	40	30	30	30	30
SDF C_{100} coefficient	80	80	80	80	80	80	60	60	60	60
Channel geomorphology										
L_{CH} (km)	28	9	14	55	26	5	29	38	46	19
Σ River lengths (km)	40	9	21	151	82	11	29	111	137	19
S_{CH} (%)	4.49	1.77	4.06	0.46	1.61	5.53	1.58	0.89	0.96	3.33
Strahler order	2	1	1	3	3	2	1	3	3	1
Shreve magnitude	2	1	1	10	6	2	1	6	7	1
D_D (km km^{-2})	0.2	0.2	0.3	0.2	0.2	0.5	0.2	0.2	0.2	0.2

Catchment descriptor	H1H018*	H2H003	H3H001	H4H005*	H4H006*	H6H003*	H6H008	H7H003	H7H004*
Climatological variables									
MAP (mm)	666	281	413	289	450	859	1336	524	566
P_{100} (mm)	109.6	114.3	113.6	103.9	212.2	169.3	99.2	123.5	99.5
Catchment geomorphology									
A (km^2)	109	743	594	29	2 878	500	39	458	28
P (km)	60	154	123	23	304	135	30	126	36
L_H (km)	23	62	52	6	110	39	11	48	16
L_C (km)	9	20	23	3	27	14	5	23	7
S (%)	41.61	37.06	23.92	43.01	29.21	25.56	40.94	23.13	31.28
Catchment variables									
Urban areas (%)	0.00	0.39	0.01	0.00	1.30	13.94	0.00	0.58	6.59
Rural areas (%)	99.57	98.67	99.72	99.62	96.81	0.45	100.00	99.26	93.24
Water bodies (%)	0.43	0.93	0.27	0.38	1.89	85.61	0.00	0.16	0.17
Weighted *CN* value	67.1	62.4	70.5	68.0	64.2	61.7	73.0	67.4	72.9
SDF C_2 coefficient	30	30	30	30	30	30	30	30	30
SDF C_{100} coefficient	60	60	60	60	60	60	60	60	60
Channel geomorphology									
L_{CH} (km)	23	60	52	6	102	38	10	47	15
Σ River lengths (km)	31	147	106	8	556	106	10	97	15
S_{CH} (%)	3.20	1.54	0.56	14.34	0.47	0.97	6.96	0.94	4.54
Strahler order	2	3	2	2	4	2	1	2	1
Shreve magnitude	2	6	4	2	22	5	1	4	1
D_D (km km^{-2})	0.3	0.2	0.2	0.3	0.2	0.2	0.3	0.2	0.5

*= Flow-gauging stations used for the calibration of Equation 7

Table A4. General information of the catchments situated in the ESC region

Catchment descriptor	T1H004*	T3H002*	T3H004	T3H005	T3H006*	T4H001*	T5H001*	T5H004*	U2H005*	U2H006	U2H011*
Climatological variables											
MAP (mm)	897	781	818	866	853	881	960	1 060	979	1 070	1 013
P_{100} (mm)	165.1	161.8	175.5	171.7	179.4	286.1	188.5	130.5	143.7	150.9	155
Catchment geomorphology											
A (km^2)	4 923	2 102	1 027	2 565	4 282	723	3 639	537	2 523	338	176
P (km)	333	226	187	299	356	131	329	123	282	108	65
L_H (km)	205	109	103	160	197	68	200	67	175	49	36
L_C (km)	99	23	50	87	113	32	85	24	70	23	18
S (%)	16.10	20.82	16.64	25.52	20.03	21.49	21.48	28.31	15.52	16.36	17.31
Catchment variables											
Urban areas (%)	6.75	5.80	0.40	3.63	2.42	0.46	0.35	0.19	0.97	0.00	22.02
Rural areas (%)	92.19	86.33	93.11	95.83	95.22	99.30	95.39	94.59	93.19	96.12	76.75
Water bodies (%)	1.06	7.87	6.49	0.54	2.36	0.23	4.25	5.22	5.84	3.88	1.23
Weighted *CN* value	70.5	66.5	70.3	69.0	71.7	69.7	70.2	68.5	68.1	75.2	72.6
SDF C_2 coefficient	10	10	10	10	10	15	10	10	10	10	10
SDF C_{100} coefficient	80	80	80	80	80	80	80	80	80	80	80
Channel geomorphology											
L_{CH} (km)	205	109	103	160	197	68	199	67	174	49	35
Σ River lengths (km)	997	409	206	641	1030	179	772	98	608	102	35
S_{CH} (%)	0.50	0.14	0.34	0.45	0.34	0.95	0.61	0.77	0.68	0.67	1.28
Strahler order	4	3	2	3	4	3	4	2	3	2	1
Shreve magnitude	21	11	6	20	25	5	18	3	16	3	1
D_D (km km^{-2})	0.2	0.2	0.2	0.3	0.2	0.2	0.2	0.2	0.2	0.3	0.2

Catchment descriptor	U2H012	U2H013*	U4H002	V1H004*	V1H009*	V2H001*	V2H002	V3H005*	V3H007	V5H002	V6H002*
Climatological variables											
MAP (mm)	954	985	911	1199	813	901	977	895	869	841	839
P_{100} (mm)	159.5	153	141.5	140	131.6	215.4	226.8	198.1	140.4	231.4	233.4
Catchment geomorphology											
A (km^2)	431	296	317	446	195	1 951	945	677	128	28 893	12 854
P (km)	99	91	88	108	62	271	148	134	66	1098	594
L_H (km)	57	51	48	42	28	188	105	86	25	505	312
L_C (km)	25	29	23	23	15	87	48	50	17	287	118
S (%)	13.33	18.35	13.74	41.39	10.96	15.26	16.15	12.94	20.22	16.24	16.97
Catchment variables											
Urban areas (%)	0.21	0.00	0.04	0.03	0.34	0.28	0.15	0.41	0.00	1.05	0.98
Rural areas (%)	98.23	89.90	90.42	99.90	91.28	90.96	90.47	87.55	92.77	93.63	94.95
Water bodies (%)	1.56	10.10	9.54	0.07	8.39	8.76	9.38	12.04	7.23	5.32	4.06
Weighted *CN* value	68.3	70.0	67.5	72.3	73.6	71.3	72.1	69.7	65.1	70.3	71.6
SDF C_2 coefficient	10	10	10	15	15	15	15	15	15	15	15
SDF C_{100} coefficient	80	80	80	50	50	50	50	50	50	50	50
Channel geomorphology											
L_{CH} (km)	57	50	48	42	28	188	105	86	25	504	312
Σ River lengths (km)	106	50	49	123	28	440	225	124	25	5370	2487
S_{CH} (%)	0.68	1.78	0.65	2.13	0.58	0.40	0.41	0.25	0.93	0.27	0.24
Strahler order	2	1	1	4	1	3	2	2	1	5	5
Shreve magnitude	3	1	1	22	1	9	3	2	1	144	79
D_D (km km^{-2})	0.2	0.2	0.2	0.3	0.1	0.2	0.2	0.2	0.2	0.2	0.2

*= Flow-gauging stations used for the calibration of Equation 7

